Acta Pharmacologica Sinica

www.nature.com/aps

ARTICLE

S-nitrosylation of Hsp90 promotes cardiac hypertrophy in mice through GSK3β signaling

Shuang Zhao[1], Tian-yu Song[1], Zi-yu Wang[2], Jie Gao[2], Jia-wei Cao[1], Lu-lu Hu[2], Zheng-rong Huang[3], Li-ping Xie[2] and Yong Ji[1,2]

Cardiac hypertrophy, as one of the major predisposing factors for chronic heart failure, lacks effective interventions. Exploring the pathogenesis of cardiac hypertrophy will reveal potential therapeutic targets. S-nitrosylation is a kind of posttranslational modification that occurs at active cysteines of proteins to mediate various cellular processes. We here identified heat shock protein 90 (Hsp90) as a highly S-nitrosylated target in the hearts of rodents with hypertrophy, and the role of Hsp90 in cardiac hypertrophy remains undefined. The S-nitrosylation of Hsp90 (SNO-Hsp90) levels were elevated in angiotensin II (Ang II)- or phenylephrine (PE)-treated neonatal rat cardiomyocytes (NRCMs) in vitro as well as in cardiomyocytes isolated from mice subjected to transverse aortic constriction (TAC) in vivo. We demonstrated that the elevated SNO-Hsp90 levels were mediated by decreased S-nitrosoglutathione reductase (GSNOR) expression during cardiac hypertrophy, and delivery of GSNOR adeno-associated virus expression vectors (AAV9-GSNOR) decreased the SNO-Hsp90 levels to attenuate cardiac hypertrophy. Mass spectrometry analysis revealed that cysteine 589 (Cys589) might be the S-nitrosylation site of Hsp90. Delivery of the mutated AAV9-Hsp90-C589A inhibited SNO-Hsp90 levels and attenuated cardiac hypertrophy. We further revealed that SNO-Hsp90 led to increased interaction of glycogen synthase kinase 3β (GSK3β) and Hsp90, leading to elevated GSK3β phosphorylation and decreased eIF2Bε phosphorylation, thereby aggravating cardiac hypertrophy. Application of GSK3β inhibitor TWS119 abolished the protective effect of Hsp90-C589A mutation in Ang II-treated NRCMs. In conclusion, this study demonstrates a critical role of SNO-Hsp90 in cardiac hypertrophy, which may be of a therapeutic target for cardiac hypertrophy treatment.

Keywords: cardiac hypertrophy; S-nitrosylation; Hsp90; GSK3β; neonatal rat cardiomyocytes; transverse aortic constriction mice

Acta Pharmacologica Sinica (2022) 43:1979–1988; https://doi.org/10.1038/s41401-021-00828-9

INTRODUCTION

Cardiac hypertrophy is characterized by increased cardiomyocyte size and thickened ventricular walls. Initially, such growth is an adaptive response to maintain cardiac function; however, under conditions of sustained stress and as time progresses, these changes become maladaptive and ultimately lead to heart failure [1]. Therapeutic solutions for cardiac hypertrophy are still limited, and understanding the underlying regulatory processes in the development of pathological hypertrophy is necessary for the development of effective therapies.

Nitric oxide (NO) has been proven to play an important role in the cardiovascular system. It is no longer thought that NO synthesized within cardiomyocytes acts only as a freely diffusible messenger. Instead, constitutive NO release operates within discrete subcellular domains either by stimulating soluble guanylate cyclase (sGC) to produce cyclic guanosine monophosphate (cGMP) or via the S-nitrosylation (SNO) of specific protein targets [2]. SNO, as a kind of posttranslational modification, occurs at reactive cysteine thiols of target proteins [3], and this modification can regulate protein function and cellular signaling by altering protein conformation, localization, activity or protein–protein interactions, thus playing a vital role in the pathogenesis of cardiovascular diseases [4–6].

Heat shock protein 90 (Hsp90), a molecular chaperone, is essential for interacting with various cochaperones and activating many signaling proteins to participate in diverse cellular processes in eukaryotic cells [7]. Posttranslational modifications of Hsp90 are important for regulating its activity, and different posttranslational modifications have been reported to affect the interaction of Hsp90 with distinct client proteins [8, 9]. Recent studies revealed that the function of Hsp90 could be regulated by S-nitrosylation [10, 11], but whether the S-nitrosylation of Hsp90 (SNO-Hsp90) might participate in cardiac hypertrophy remains unclear.

In this study, we demonstrated the critical role of SNO-Hsp90 in cardiac hypertrophy. We found that SNO-Hsp90 levels were significantly elevated in hypertrophic cardiomyocytes, and these increased SNO-Hsp90 levels were caused by the reduced expression of S-nitrosoglutathione reductase (GSNOR). The SNO-Hsp90 at cysteine 589 (Cys589) promoted the interaction of Hsp90 with glycogen synthase kinase 3β (GSK3β), leading to the incremental phosphorylation of GSK3β, which accelerated cardiac hypertrophy. Administration of Cys589-mutated AAV9-Hsp90

[1]Key Laboratory of Cardiovascular and Cerebrovascular Medicine, Nanjing Medical University, Nanjing 210029, China; [2]Key Laboratory of Targeted Intervention of Cardiovascular Disease, Collaborative Innovation Center for Cardiovascular Disease Translational Medicine, Nanjing Medical University, Nanjing 210029, China and [3]Department of Cardiology, The First Affiliated Hospital of Xiamen University, Xiamen 361003, China
Correspondence: Yong Ji (yongji@njmu.edu.cn) or Li-ping Xie (lipingxie@njmu.edu.cn) or Zheng-rong Huang (huangzhengrong@xmu.edu.cn)
These authors contributed equally: Shuang Zhao, Tian-yu Song.

Received: 26 July 2021 Accepted: 18 November 2021
Published online: 21 December 2021

inhibited SNO-Hsp90 and mitigated the interaction of Hsp90 with GSK3β to improve hypertrophic symptoms. Our findings may provide a therapeutic strategy for treating pathological cardiac hypertrophy.

MATERIALS AND METHODS

Animals

Adult male C57BL/6J mice were obtained from the Experimental Animal Center of Nanjing Medical University. Twelve-week-old male Wistar Kyoto rats (WKY) and spontaneously hypertensive rats (SHR) were obtained from Shanghai SLAC Laboratory Animal Co. Ltd. Food and water were provided *ad libitum* throughout the experiments. The animals were housed under standard animal room conditions (temperature 21 ± 1 °C; humidity 55%–60%; 12-h light/dark cycles).

Four-week-old male C57BL/6J mice were injected through the tail vein with 1.5×10^{11} genome copies of adeno-associated virus serotype 9 (AAV9) carrying green fluorescent protein (GFP), GSNOR, wild-type Hsp90 (Hsp90-WT) or Cys589 SNO site-mutated Hsp90 (Hsp90-C589A) to achieve the myocardial overexpression of these proteins. The AAV9-GFP, AAV9-GSNOR, AAV9-HA-Hsp90-WT and AAV9-HA-Hsp90-C589A constructs were generated by Kunshan Renyuan Biotechnology Company (Suzhou, China).

A mouse model of cardiac hypertrophy was established using transverse aortic constriction (TAC) surgery on 8-week-old male C57BL/6J mice and AAV9-treated mice.

All the animal experiments were approved by the Committee on Animal Care of Nanjing Medical University (approval no. NJMU-1811010) and were conducted according to the NIH Guidelines for the Care and Use of Laboratory Animals. All the studies involving animals were reported in accordance with the ARRIVE guidelines.

TAC surgery

Surgeries were performed according to previously published protocols [12]. Briefly, 8-week-old male C57BL/6J mice or AAV9-treated mice were anesthetized and placed in a supine position. A midline cervical incision was made to expose the trachea. After successful endotracheal intubation, the cannula was connected to a volume cycled rodent ventilator. The chest was opened, and the thoracic aorta was identified. A 7-0 silk suture was placed around the transverse aorta and tied around a 26-gauge blunt needle, which was subsequently removed. At predetermined time points (2 and 4 weeks), the surviving mice were sacrificed, and the hearts were quickly harvested, weighed, and stored in cold (4 °C) buffer for other experiments.

Echocardiography

Cardiac function was assessed by echocardiography with a 30-MHz small animal color ultrasonic diagnostic apparatus (VisualSonic Vevo 2100). Mice were anesthetized with 1.5% isoflurane and placed on a heating table in a supine position. Two-dimensional and M-mode images were recorded in a short-axis view from the mid-left ventricle at the tips of the papillary muscles. The calculated left ventricular (LV) mass, diastolic interventricular septum (IVS,d), diastolic LV posterior wall (LVPW,d), ejection fraction (EF) and fractional shortening (FS) were calculated with VEVO Analysis software (version 2.2.3).

Neonatal rat cardiomyocyte (NRCM) culture and treatment

Neonatal Sprague–Dawley rats were obtained from the Experimental Animal Center of Nanjing Medical University. NRCMs were isolated from the ventricles of 1–3-day-old neonatal rats by enzymatic digestion. Briefly, each pup was placed on a 37 °C temperature-controlled pad. The hearts were quickly harvested, washed, and minced in serum-free DMEM. The myocardial cells were dispersed by incubation with 0.25% trypsin-EDTA, which were then mixed by intermittent pipetting and stirring at 37 °C in a water bath for 3 min. The cell suspension was allowed to stand for 1 min. The supernatant containing single cells was collected into 15-mL tubes on ice, to which 7 mL media supplemented with 10% fetal bovine serum (FBS) was added, and the digestion step was repeated five to ten times until the tissue was completely digested. The cell suspensions from each digestion were pooled and centrifuged at 2000 r/min for 10 min at 4 °C. The cells were suspended in DMEM supplemented with 10% FBS and precultured in a humidified incubator (95% air and 5% CO_2) for 3 h to remove the fibroblasts. The nonadherent cardiomyocytes were planted in another dish. Thirty-six hours after planting, the NRCMs were stimulated with angiotensin II (Ang II, 1 μM), phenylephrine (PE, 50 μM) or the corresponding vehicle.

Isolation of adult mouse cardiomyocytes

Cardiomyocytes were isolated from sham or TAC-operated mice through Langendorff perfusion as described previously [13]. Briefly, mouse hearts were quickly removed from mouse chests after anesthesia by isoflurane and hung on a Langendorff perfusion system; the hearts were perfused with Ca^{2+}-free bicarbonate-based buffer containing 120 mM NaCl, 5.4 mM KCl, 1.2 mM $MgSO_4$, 1.2 mM NaH_2PO_4, 5.6 mM glucose, 20 mM $NaHCO_3$, 10 mM 2,3-butanedione monoxime, and 5 mM taurine for 5 min. Enzymatic digestion was initiated by adding collagenase type II (Worthington, 0.5 mg/mL each) and protease type XIV (Sigma, 0.02 mg/mL) to the perfusion buffer and continued for 15 min. When the hearts became swollen, Ca^{2+} (50 mM) was added to the enzyme solution and reperfused for 10 min. The left ventricles were then quickly removed, cut into several chunks, and gently aspirated. The cell pellets were resuspended for a 3-step Ca^{2+} restoration procedure (125, 250, 500 mM Ca^{2+}). The supernatants containing the dispersed cardiomyocytes were filtered into a sterilized tube and gently centrifuged at 500 r/min for 1 min to harvest the cardiomyocytes.

Mass spectrometry (MS) to identify S-nitrosylated proteins

Liquid chromatography with tandem MS (LC/MS) analysis was performed by the Institute of Biophysics, Chinese Academy of Sciences. Purified heart proteins from WKY rats and SHR were blocked with N-ethylmaleimide and labeled with biotin-maleimide. Then, the biotinylated proteins were immunoprecipitated with streptavidin-agarose and trypsinized (using a 1:50 ratio of protein:trypsin) for LC/MS analysis. Peptides were separated using the NanoLC 1D Plus system. Eluting peptide cations were ionized by nanospray and analyzed using an LTQ-Orbitrap XL mass spectrometer (Thermo Fisher Scientific). Tandem mass spectra were searched against the UniProt rat proteome database using SequestHT.

Immunoprecipitation

Cells or heart tissues were harvested and lysed as previously described [14]. Antibodies specific for HA (Santa Cruz, CA, USA) were added to the supernatants and incubated. Immune complexes were then precipitated with protein A + G-agarose beads. Bound proteins were eluted by boiling with loading buffer and analyzed by Western blotting with an anti-GSK3β antibody (CST, MA, USA).

Plasmid transfection

The plasmid pcDNA-HA-Hsp90 was purchased from Addgene (Cambridge, MA) and was called Hsp90-WT. A single mutation of Cys589 to Ala (Hsp90-C589A, Haibio, Shanghai, China) was confirmed by DNA sequencing. Adenoviral (ad) constructs encoding GSNOR, HA-Hsp90-WT and HA-Hsp90-C589A were

purchased from Hanbio (Shanghai, China). HEK293 cells were transfected with expression vectors using Lipofectamine 3000 reagent (Invitrogen). NRCMs were infected with adPDC (plasmid-derived control), adGSNOR, ad-Hsp90-WT or ad-Hsp90-C589A.

Biotin switch assay of SNO

SNO-Hsp90 levels were determined by biotin switch assay with the S-nitrosylation Protein Detection Assay Kit (Cayman Chemical; item No. 10006518) as described previously [6]. In brief, cell lysates were incubated with blocking buffer for 30 min to block free thiols, and the proteins were precipitated with cold acetone. Then, S-nitrosothiols in proteins were reduced to free thiols with reducing buffer (vitamin C, Vc) and labeled with biotin with labeling buffer. Samples not incubated with reducing buffer were used as negative controls (−Vc). The biotinylated proteins were purified by incubation with NeutrAvidin Plus UltraLink Resin (Thermo Scientific) overnight at 4 °C, followed by SDS–PAGE analysis with anti-Hsp90 or anti-HA antibodies (Santa Cruz, CA, USA).

Western blotting

Equal amounts of protein were resolved by 8% or 10% SDS–PAGE, and Western blotting analysis was performed as previously described [15]. Primary antibodies included anti-Hsp90 antibody (Santa Cruz, CA, USA), anti-GSNOR antibody (Abcam, Cambridge, UK), anti-Trx antibody (Abcam, Cambridge, UK), anti-eNOS antibody (CST, MA, USA), anti-HA antibody (Santa Cruz, CA, USA), anti-iNOS antibody (CST, MA, USA), anti-GSK3β antibody (CST, MA, USA), anti-p-GSK3β antibody (CST, MA, USA), anti-eIF2Bε antibody (CST, MA, USA), anti-p-eIF2Bε (CST, MA, USA), and anti-GAPDH (CST, MA, USA). The band intensities were analyzed by Image-Pro Plus 8.0 software.

Immunofluorescence staining

Cells were washed with phosphate buffered saline (PBS), fixed with 4% paraformaldehyde, permeabilized with 0.3% Triton X-100, blocked in 3% bovine serum albumin (BSA), and then incubated overnight at 4 °C with an anti-α-actinin antibody (Abcam, Cambridge, UK). Secondary fluorescent antibodies (Alexa 594; Life Technologies, Carlsbad, USA) were incubated for 1 h at room temperature, and DAPI (Santa Cruz, CA, USA) was used for nuclear counterstaining. The samples were imaged with confocal microscopy (Zeiss LSM 410, Oberkochen, Germany).

RNA analysis

Atrial natriuretic peptide (ANP), brain natriuretic peptide (BNP) and β-myosin heavy chain (β-MHC) mRNA expression was quantified by real-time polymerase chain reaction (RT-PCR) with the following forward (F) and reverse (R) primers: rat ANP (F) 5′-ATCTGCCCTCTTGAAAAGCA-3′, (R) 5′-GGATCTTTTGCGATCTGCTC-3′; rat BNP (F) 5′-ATCGGCGCAGTCAGTCGCTT-3′, (R) 5′-GGTGGTC CCAGAGCTGGGGAA-3′; rat β-MHC (F), 5′-AGATCGAGGACCTGAT GGTG-3′, (R) 5′-GATGCTCTTCCCAGTTGAGC-3′; rat 18S (F) 5′-AGT CCCTGCCCTTTGTACACA-3′, (R) 5′-CGATCCGAGGGCCTCACTA-3′; mouse ANP (F) 5′-ATTGACAGGATTGGAGCCCAGAGT-3′, (R) 5′-TGA CACACCACAAGGGCTTAGGAT-3′; mouse BNP (F) 5′-CTCAAGCTG CTTTGGGCACAAGAT-3′; (R) 5′-AGCCAGGAGGTCTTCCTACAACAA-3′; mouse β-MHC (F) 5′-TTTGATGTGCTGGGCTTCAC-3′, (R) 5′-TGAC ATACTCGTTGCCCACT-3′; mouse GAPDH (F) 5′- GACCTCATGGCCTA CATGGC-3′, and (R) 5′-GCCCCTCCTGTTATTATGGGG-3′.

Measurement of NO levels

NRCMs were infected with GSNOR adenovirus to overexpress GSNOR and treated with or without Ang II (1 μM) for 24 h. Then, the concentration of NO in the cardiomyocytes was measured by a total NO assay kit (Beyotime Company, Shanghai, China).

Statistical analysis

All the data are presented as the mean ± standard error of the mean. The distribution of the data was first analyzed using the Shapiro–Wilk test for analysis of normality. Unpaired two-tailed Student's *t* test was used for comparisons between two groups when data passed normality and equal variance test; otherwise, Mann–Whitney *U* test was used. Differences among groups were evaluated using one-way ANOVA followed by Tukey's *post hoc* test. The comparison of indicators between two groups at different time points was performed with two-way ANOVA followed by Bonferroni's multiple comparisons test. For all tests, *P* values lower than 0.05 were considered statistically significant. All the statistical analyses were performed with GraphPad Prism version 8.01 (GraphPad Software Inc., San Diego, CA, USA).

RESULTS

SNO-Hsp90 levels are increased in cardiac hypertrophy

To determine whether protein SNO is involved in cardiac hypertrophy, we first performed biotin switch analysis to detect protein SNO levels in hypertrophic hearts from 12-week-old SHR and found that the levels of whole S-nitrosylated protein (SNO protein) were obviously increased in SHR hearts compared with WKY control hearts (Fig. 1a). To further explore the potential S-nitrosylated protein targets that may be involved in the process of cardiac hypertrophy, we scanned the S-nitrosylated proteins by MS and identified Hsp90 as one of the highly S-nitrosylated proteins in hypertrophic hearts (Fig. 1b). Then, we performed biotin switch analysis to confirm that the level of S-nitrosylated Hsp90 (SNO-Hsp90) was increased in NRCMs treated with Ang II (Fig. 1c) or PE (Fig. 1d). Moreover, we found that the SNO-Hsp90 levels were significantly increased in cardiomyocytes isolated from mice subjected to TAC (Fig. 1e). These results indicate that SNO-Hsp90 may participate in the development of cardiac hypertrophy.

SNO-Hsp90 levels are regulated by GSNOR during cardiac hypertrophy

To investigate the regulatory mechanisms of protein SNO during the development of cardiac hypertrophy, first, C57BL/6J mice were subjected to TAC surgery, and then, M-mode echocardiography was used to assess the process of hypertrophy. Hypertrophic symptoms emerged at 2 weeks after TAC surgery, as evidenced by elevated IVS,d and LVPW,d thickness values (Fig. 2a) as well as increased LV internal diastolic diameter (LVID,d) and LV internal systolic diameter (LVID,s) (Supplementary Fig. 1a, b). In addition, the heart weight (HW)/body weight (BW) ratios were significantly increased at 4 weeks after TAC but not at 2 weeks (Fig. 2b). Cellular SNO is regulated by NO synthase, GSNOR and thioredoxin (Trx). NO synthase (NOS) can enhance the level of SNO, while GSNOR and Trx can denitrosylate SNO [16]. Then, we detected the expression of these enzymes and found that GSNOR expression was decreased at both 2 and 4 weeks after TAC surgery and that inducible NOS (iNOS) expression increased only at 4 weeks after TAC surgery (Fig. 2c, d). Meanwhile, the expression of GSNOR was obviously decreased while the expression of iNOS was not significantly changed in NRCMs after Ang II treatment for 2 h (Fig. 2e). GSNOR is reported to play an important role in regulating protein SNO levels. $GSNOR^{-/-}$ mice exhibit substantial increases in whole-cell protein SNO [17]. To further investigate whether the elevated SNO-Hsp90 levels were due to reduced GSNOR expression, we used adenovirus to overexpress GSNOR in NRCMs. The biotin switch results showed that the SNO-Hsp90 levels were strongly enhanced after Ang II treatment and were obviously inhibited in adGSNOR-treated cells (Fig. 2f). Moreover, GSNOR overexpression significantly inhibited the increase in NO content induced by Ang II stimulation (Supplementary Fig. 2a). Furthermore, the ANP, BNP and β-MHC mRNA levels were dramatically

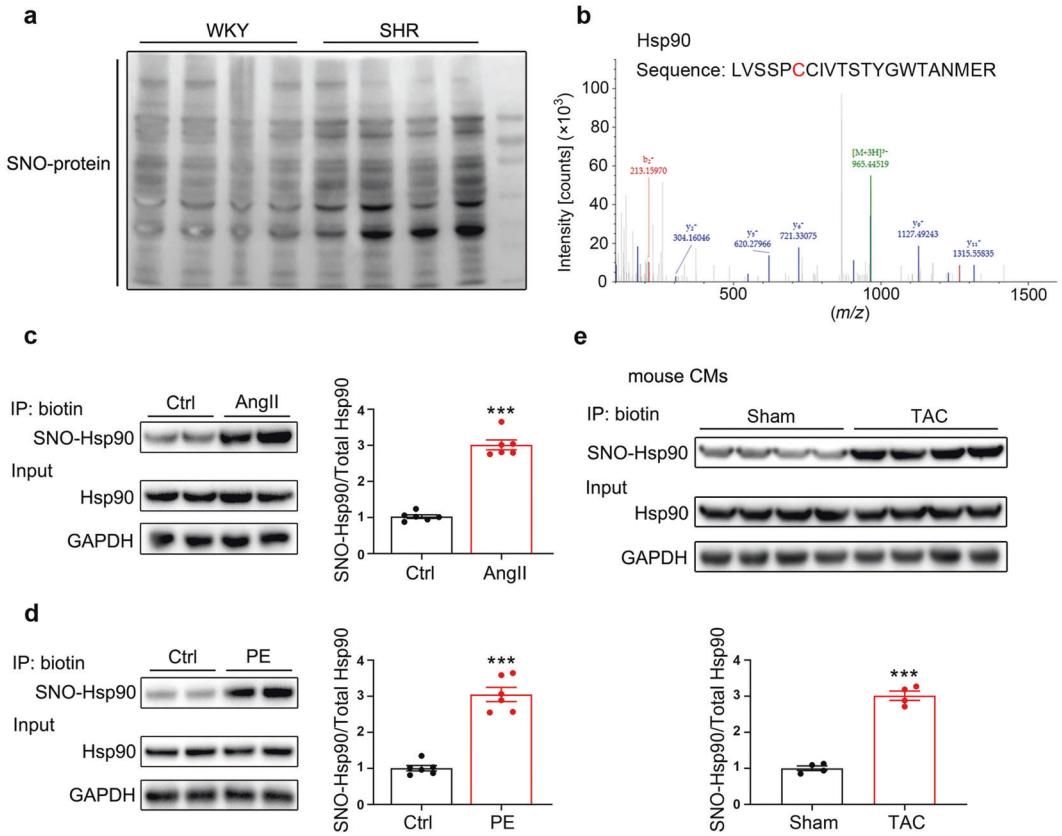

Fig. 1 SNO-Hsp90 levels are significantly increased in hypertrophic cardiomyocytes. a S-Nitrosylated proteins in myocardial tissues from 12-week-old Wistar Kyoto (WKY) rats or spontaneously hypertensive rats (SHR) were purified by biotin switch, followed by Western blotting analysis. ($n = 4$). **b** Liquid chromatography-tandem mass spectrometry (LC–MS/MS) scans of S-nitrosylated proteins in hearts from SHR were performed. Representative LC–MS/MS spectra showed a target modification site (Cys589) in the peptide fragmentation of Hsp90. **c** The SNO-Hsp90 levels in angiotensin II (Ang II)-treated (1 μM, 24 h) neonatal rat cardiomyocytes (NRCMs) were detected by biotin switch assay. ($n = 6$, $^{***}P < 0.001$ vs. Ctrl). **d** The SNO-Hsp90 levels in phenylephrine (PE)-treated (50 μM, 24 h) NRCMs were detected by biotin switch assay. ($n = 6$, $^{***}P < 0.001$ vs. Ctrl). **e** Eight-week-old C57BL/6J mice were subjected to sham or transverse aortic constriction (TAC) surgery. The SNO-Hsp90 levels in cardiomyocytes isolated from mice at 4 weeks after surgery were detected by biotin switch assay. ($n = 4$, $^{***}P < 0.001$ vs. Sham).

decreased in adGSNOR-treated cells after Ang II treatment for 24 h compared with adPDC-treated cells (Supplementary Fig. 2b). The cell surface area of NRCMs was also decreased in adGSNOR-treated cells compared with adPDC-treated cells after Ang II treatment (Supplementary Fig. 2c). Moreover, we constructed AAV9 to overexpress GSNOR in the heart, and these mice were subjected to TAC to induce cardiac hypertrophy. The biotin switch analysis showed that the SNO-Hsp90 levels were significantly increased at 4 weeks after TAC surgery, and dramatically decreased in AAV9-GSNOR-treated mice (Fig. 2g). Moreover, the hypertrophic symptoms were obviously alleviated by AAV9-GSNOR treatment after TAC (Supplementary Fig. 3a–c). These results suggest that in pressure-overloaded hypertrophic hearts, SNO-Hsp90 in cardiomyocytes is regulated by GSNOR.

Cys589 is the SNO site of Hsp90, and its mutation suppresses cardiac hypertrophy

MS analysis showed that Cys589 may be the SNO site of Hsp90 (Fig. 1b). For further verification, we constructed mutagenesis plasmids by substituting the Cys589 of Hsp90 with the non-nitrosylable alanine. Mutated Hsp90 was expressed in HEK293 cells, and the SNO-Hsp90 levels were determined by biotin switch assay after NO donor (SNP, 100 μM) treatment. The results showed that mutation of Cys589 to Ala (C589A) abolished the elevated SNO-Hsp90 levels induced by SNP (Supplementary Fig 4a), indicating that Cys589 is the SNO site of Hsp90. Then, Hsp90-WT and Hsp90-C589A adenovirus expression vectors were constructed for further research in NRCMs. Compared with Hsp90-WT, Hsp90-C589A abolished the increase in the SNO-Hsp90 levels after Ang II treatment (Fig. 3a). In addition, the RT-PCR results showed that compared with Hsp90-WT-infected NRCMs, Hsp90-C589A-infected NRCMs exhibited significantly attenuated increases in the ANP, BNP and β-MHC levels after Ang II or PE treatment (Fig. 3b, c). Moreover, the cell surface area of NRCMs was also decreased in Hsp90-C589A-infected cells treated with Ang II or PE compared with Hsp90-WT-infected cells (Fig. 3d, e).

To further investigate the effect of the Cys589 mutation in vivo, we used AAV9 to overexpress Hsp90-WT or Hsp90-C589A in the hearts of C57BL/6J mice, which were then subjected to sham or TAC surgery. Morphological analysis and hematoxylin-eosin staining of the heart cross-sectional areas showed that TAC-induced cardiac hypertrophy was significantly suppressed in AAV9-Hsp90-C589A-treated mice (Fig. 4a). The Hsp90-C589A mutation markedly decreased the enhancive IVS,d and LVPW,d and increased the declining EF and FS induced by TAC (Fig. 4b–f). Moreover, the HW/BW ratios and ANP, BNP and β-MHC mRNA levels demonstrated significant cardiac hypertrophy in AAV9-Hsp90-WT-treated TAC mice, but not in AAV9-Hsp90-Cys589A-treated mice (Fig. 4g, h). These results show that inhibition of SNO-Hsp90 by Cys589 mutation weakens the effect of hypertrophic stimulation both in vivo and in vitro.

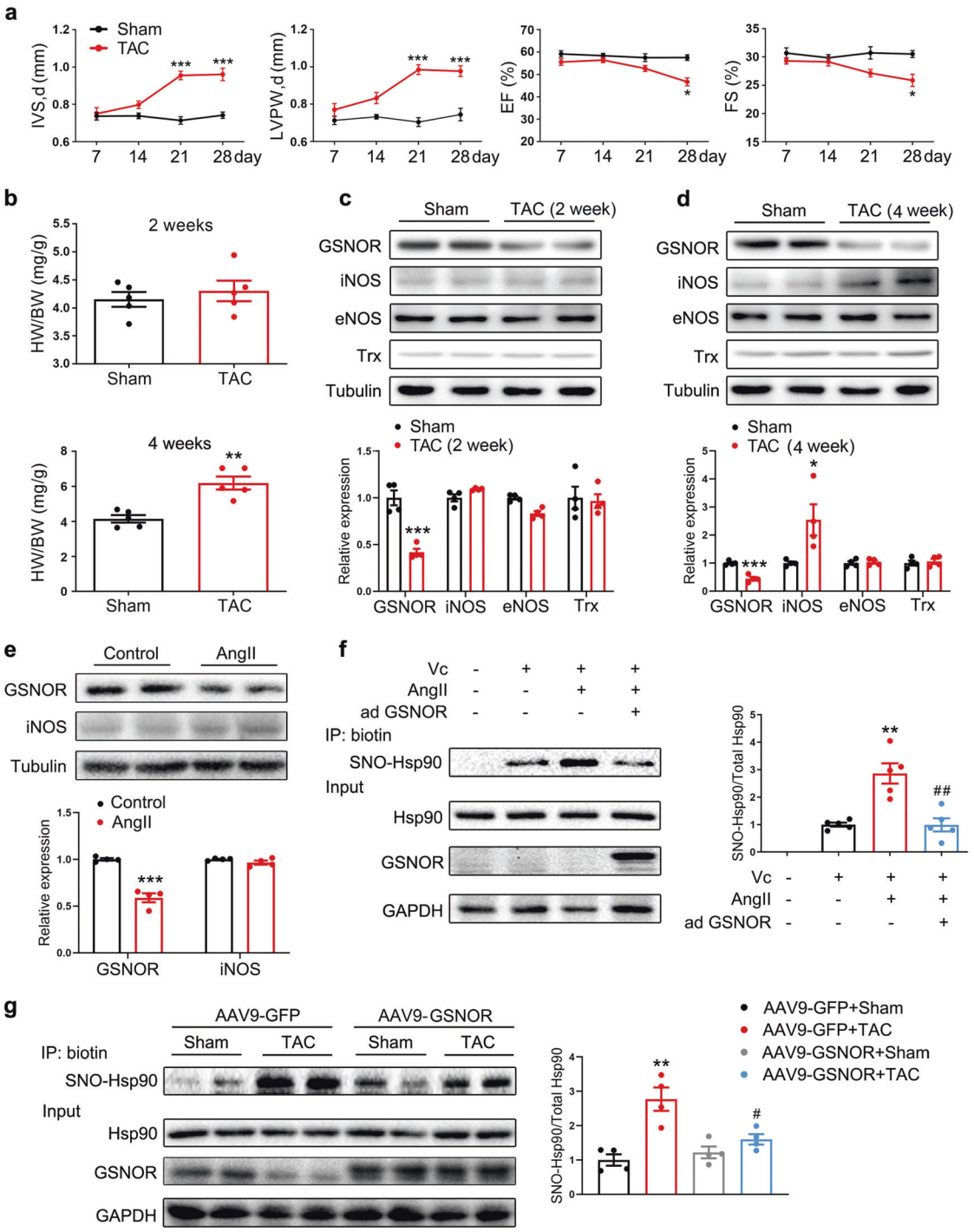

Fig. 2 Increases in the SNO-Hsp90 levels are mediated by decreased GSNOR expression during cardiac hypertrophy. a–d Eight-week-old C57BL/6J mice were subjected to sham or TAC surgery. **a** The diastolic interventricular septum (IVS,d), diastolic left ventricular posterior wall (LVPW,d), ejection fraction (EF) and fractional shortening (FS) were detected by echocardiography at 7, 14, 21 and 28 days after the operation. ($n = 5$, $^{*}P < 0.05$, $^{***}P < 0.001$ vs. Sham). **b** The heart weight (HW)/body weight (BW) ratios were calculated at 2 and 4 weeks after the operation. ($n = 5$, $^{**}P < 0.01$ vs. Sham). **c** Western blotting analysis of the levels of S-nitrosoglutathione reductase (GSNOR), inducible NOS (iNOS), endothelial NOS (eNOS) and thioredoxin (Trx) in the myocardial tissues of mice at 2 weeks after surgery. ($n = 4$, $^{***}P < 0.001$ vs. Sham). **d** Western blotting analysis of the levels of GSNOR, iNOS, eNOS and Trx in the myocardial tissues of mice at 4 weeks after surgery. ($n = 4$, $^{*}P < 0.05$, $^{***}P < 0.001$ vs. Sham). **e** NRCMs were treated with Ang II (1 μM) for 2 h. The expression of GSNOR and iNOS was detected by Western blotting analysis ($n = 4$, $^{***}P < 0.001$ vs. Control). **f** NRCMs were infected with GSNOR adenovirus (adGSNOR) for 24 h, followed by Ang II treatment for another 24 h. The SNO-Hsp90 levels were detected by biotin switch assay. No vitamin C (−Vc) was used as a negative control. ($n = 5$, $^{**}P < 0.01$ vs. +Vc, $^{\#\#}P < 0.01$ vs. +Vc+Ang II). **g** The SNO-Hsp90 levels in the myocardial tissues from mice at 4 weeks after surgery and treated with AAV9-GSNOR. ($n = 4$, $^{**}P < 0.01$ vs. AAV9-GFP + Sham, $^{\#}P < 0.05$ vs. AAV9-GFP + TAC).

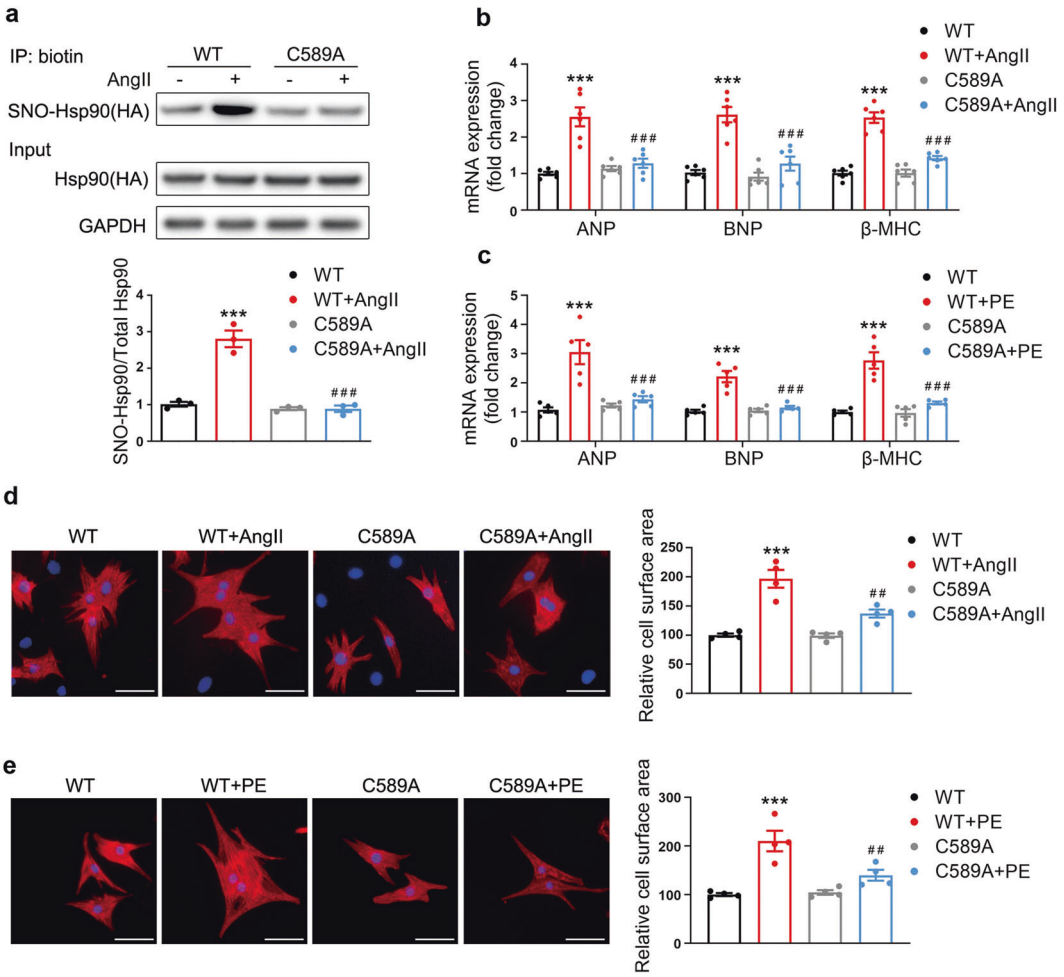

Fig. 3 Inhibition of SNO-Hsp90 levels by Cys589 mutation alleviates hypertrophy in NRCMs. a NRCMs were infected with HA-Hsp90-WT or HA-Hsp90-C589A adenovirus for 24 h and subsequently treated with Ang II (1 μM) for another 24 h. The SNO-Hsp90 levels were detected by biotin switch assay ($n = 3$, $^{***}P < 0.001$ vs. WT, $^{###}P < 0.001$ vs. WT + Ang II). **b** NRCMs were infected with HA-Hsp90-WT or HA-Hsp90-C589A adenovirus for 24 h and subsequently treated with Ang II (1 μM) for another 24 h. The mRNA levels of atrial natriuretic peptide (ANP), brain natriuretic peptide (BNP) and β-myosin heavy chain (β-MHC) were detected with real-time polymerase chain reaction (RT-PCR) ($n = 6$, $^{***}P < 0.001$ vs. WT, $^{###}P < 0.001$ vs. WT + Ang II). **c** NRCMs were infected with HA-Hsp90-WT or HA-Hsp90-C589A adenovirus for 24 h and subsequently treated with PE (50 μM) for another 24 h. The mRNA levels of ANP, BNP and β-MHC were detected with RT-PCR. ($n = 5$, $^{***}P < 0.001$ vs. WT, $^{###}P < 0.001$ vs. WT + PE). **d** NRCMs were infected with HA-Hsp90-WT or HA-Hsp90-C589A adenovirus for 24 h and subsequently treated with Ang II (1 μM) for another 24 h. Representative images of NRCMs stained with α-actinin (red) and DAPI (blue) and quantification of the average cell surface area. (Scale bar = 50 μm, $n = 4$, $^{***}P < 0.001$ vs. WT, $^{##}P < 0.01$ vs. WT + Ang II). **e** NRCMs were infected with HA-Hsp90-WT or HA-Hsp90-C589A adenovirus for 24 h and subsequently treated with PE (50 μM) for another 24 h. Representative images of NRCMs stained with α-actinin (red) and DAPI (blue) and quantification of the average cell surface area. (Scale bar = 50 μm, $n = 4$, $^{***}P < 0.001$ vs. WT, $^{##}P < 0.01$ vs. WT + PE).

SNO-Hsp90 at Cys589 promotes cardiac hypertrophy through the GSK3β/eIF2Bε signaling pathway

We further explored the mechanism by which SNO-Hsp90 participates in cardiac hypertrophy. GSK3β, one of the molecular chaperones of Hsp90, has been implicated in the development of cardiac hypertrophy [18, 19]. Co-immunoprecipitation showed that Ang II facilitated GSK3β binding to Hsp90 in Hsp90-WT-infected NRCMs, while this interaction was attenuated by Cys589 mutation (Fig. 5a). Moreover, the levels of phosphorylated GSK3β in Hsp90-WT-infected NRCMs were increased by Ang II stimulation, and this effect was suppressed by Cys589 mutation (Fig. 5b). Then, we assessed the phosphorylation of eIF2Bε, a downstream target of GSK3β involved in cardiac hypertrophy. Consistently, the Cys589 mutation abolished the Ang II-induced reduction in eIF2Bε phosphorylation in NRCMs. However, the GSK3β inhibitor TWS119 abolished the effect of the Cys589 mutation (Fig. 5c). Furthermore, the Cys589 mutation suppressed the Ang II-induced increased ANP, BNP and β-MHC mRNA levels, and this effect was abolished by TWS119 treatment (Fig. 5d). However, TWS119 had no effect on SNO-Hsp90 or the interaction between Hsp90 and GSK3β in NRCMs (Supplementary Fig. 5a, b). Accordingly, the SNO-Hsp90 at Cys589 participates in the development of cardiac hypertrophy through the GSK3β/eIF2Bε signaling pathway. Furthermore, in vivo experiments showed that the Cys589 mutation abolished the increase in cardiac SNO-Hsp90 levels after TAC surgery (Fig. 6a). Moreover, the binding of Hsp90 and GSK3β and the phosphorylation of GSK3β were significantly suppressed in AAV9-Hsp90-C589A-treated mice compared with AAV9-Hsp90-WT-treated mice after TAC surgery (Fig. 6b, c). These results indicate that SNO-Hsp90 at Cys589 participates in cardiac hypertrophy through the GSK3β signaling pathway.

DISCUSSION

Our results demonstrated that the SNO-Hsp90 levels were obviously increased in Ang II- or PE-treated cardiomyocytes and

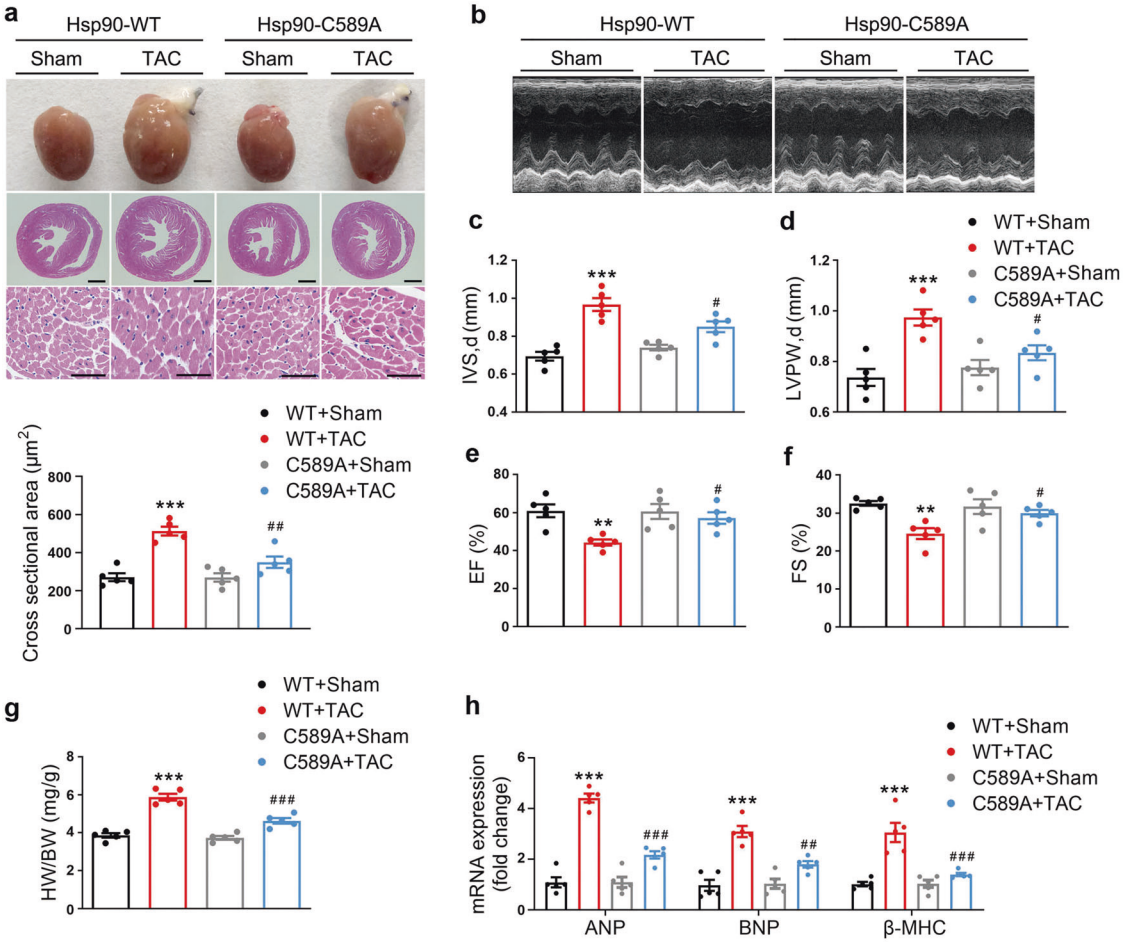

Fig. 4 Hsp90 Cys589 mutation mitigates TAC-induced cardiac hypertrophy. Four-week-old C57BL/6J mice were intravenously injected with AAV9-HA-Hsp90-WT (WT) or AAV9-HA-Hsp90-C589A (C589A). After 4 weeks, these mice were subjected to sham or TAC surgery. **a** Histological sections of myocardial tissues from AAV9-HA-Hsp90-WT- or AAV9-HA-Hsp90-C589A-treated mice at 4 weeks after surgery were stained with hematoxylin and eosin (second and third rows). The cross-sectional area of cardiomyocytes was quantified. (Scale bar = 200 μm in the second row, scale bar =50 μm in the third row, $n = 5$, $^{***}P < 0.001$ vs. WT + Sham, $^{\#\#}P < 0.01$ vs. WT + TAC). Representative images of echocardiography (**b**) and the calculation of IVS,d (**c**), LVPW,d (**d**), EF (**e**) and FS (**f**) at 4 weeks after surgery. ($n = 5$, $^{**}P < 0.01$, $^{***}P < 0.001$ vs. WT + Sham, $^{\#}P < 0.05$ vs. WT + TAC). **g** The heart weight (HW)/body weight (BW) ratios were calculated at 4 weeks after surgery. ($n = 5$, $^{***}P < 0.001$ vs. WT + Sham, $^{\#\#\#}P < 0.001$ vs. WT + TAC). **h** The cardiac mRNA levels of ANP, BNP and β-MHC were detected by RT-PCR at 4 weeks after surgery. ($n = 5$, $^{***}P < 0.001$ vs. WT + Sham, $^{\#\#}P < 0.01$, $^{\#\#\#}P < 0.001$ vs. WT + TAC).

in hearts of rodents with hypertrophy, which was due to the reduction in GSNOR expression during the development of cardiac hypertrophy. We showed that the SNO site of Hsp90 was Cys589 and that its SNO could promote the interaction of GSK3β and Hsp90, leading to the enhanced phosphorylation of GSK3β and aggravating cardiac hypertrophy. The inhibition of SNO-Hsp90 levels by Cys589 mutation improved cardiac hypertrophy both in vitro and in vivo. These data reveal a novel pathway related to cardiac hypertrophy, providing a potential target for therapeutic intervention.

Cardiac remodeling is a complex and organic pathological process characterized by hypertrophy, fibrosis and apoptosis, ultimately leading to heart failure. Although multiple molecular mechanisms have been implicated in the development of cardiac remodeling, effective therapeutic strategies for preventing or reversing pathological progression are still limited. Further exploration of the regulatory mechanism is essential for the discovery of novel intervention targets.

SNO, a new mechanism of protein posttranslational modification, has been reported to be involved in different physiological and pathological processes, especially in the nervous and cardiovascular systems [20, 21]. Our group and other groups recently reported that SNO of muscle LIM protein [6] and phospholamban [22] could aggravate cardiac hypertrophy. Here, our data revealed another S-nitrosylated protein target, Hsp90, that participated in the process of cardiac hypertrophy. Hsp90 is a member of the molecular chaperone family that is widely expressed in bacteria and all eukaryotes, and it functionally interacts with cofactors to promote conformational maturation to carry out biological functions [23]. The function of Hsp90 can be regulated by posttranslational modifications, such as phosphorylation [24], acetylation [9], ubiquitination [25] and SNO [11], allowing it to further participate in various cellular processes. There are reports regarding the role of Hsp90 in the cardiovascular system [26, 27]. However, Hsp90 has a contradictory effect on cardiac remodeling. Eschricht et al. showed that inhibition of Hsp90 aggravated LV failure by inhibiting capillary growth [28], while Marunouchi et al. found that Hsp90 inhibition could improve cardiac fibrosis [29]. Tamura et al. found that inhibition of Hsp90 attenuated the development of heart failure after myocardial infarction [30], suggesting an undefined effect of Hsp90 in cardiac remodeling. Our recent study showed that the SNO-Hsp90 in fibroblasts contributed to cardiac fibrosis under pathological conditions, and we demonstrated that the SNO of Cys589 of

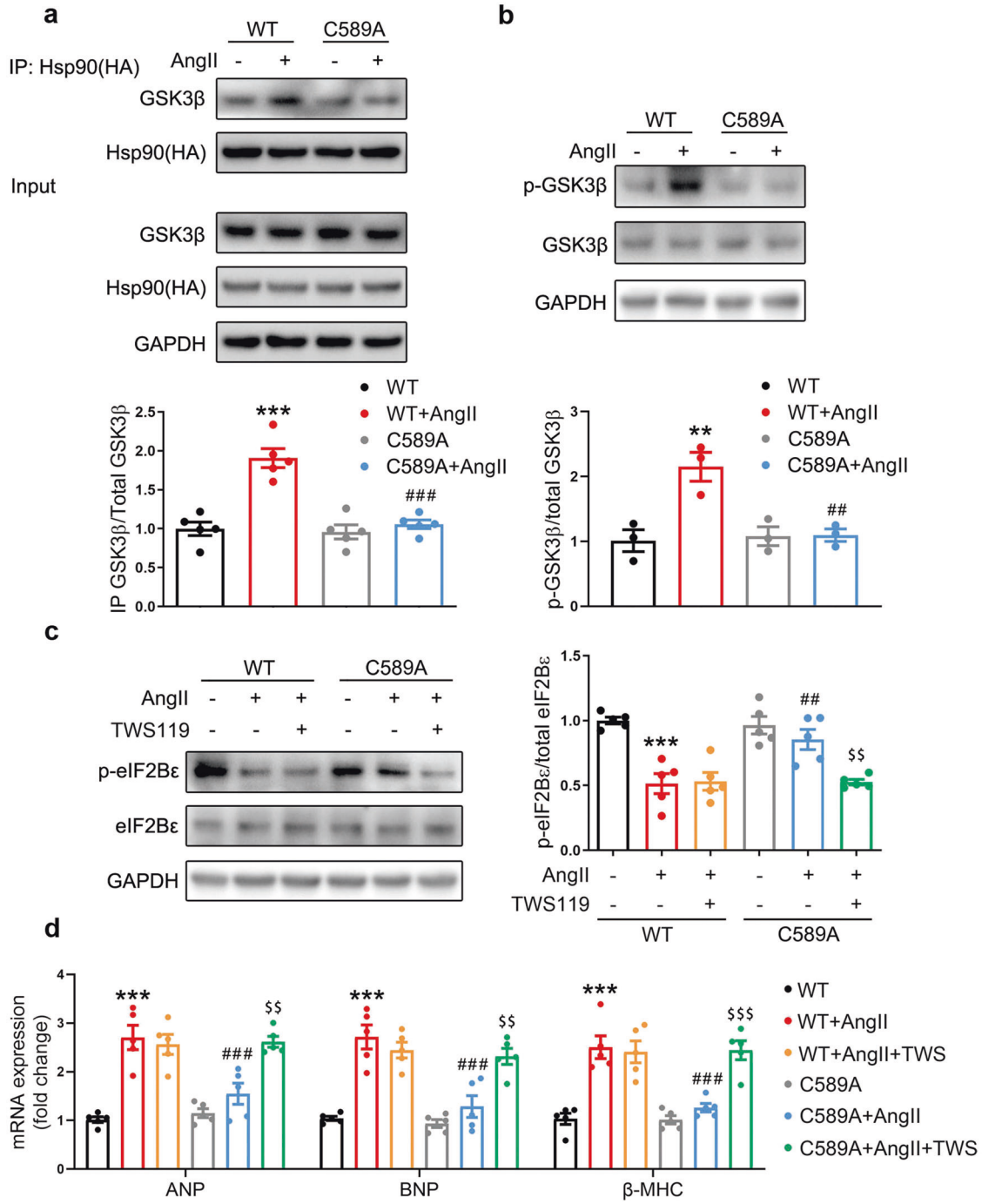

Fig. 5 SNO-Hsp90 at Cys589 aggravates cardiac hypertrophy via GSK3β signaling in NRCMs. a, **b** NRCMs were infected with HA-Hsp90-WT (WT) or HA-Hsp90-C589A (C589A) adenovirus for 24 h and subsequently treated with Ang II (1 μM, 24 h). **a** Lysates from NRCMs were immunoprecipitated with an anti-HA antibody and blotted with an anti-GSK3β and anti-HA antibody. An aliquot of total lysate was analyzed for GSK3β and HA expression. ($n = 5$, $^{***}P < 0.001$ vs. WT, $^{\#\#\#}P < 0.001$ vs. WT + Ang II). **b** The levels of GSK3β and p-GSK3β were detected by Western blotting. ($n = 3$, $^{**}P < 0.01$ vs. WT, $^{\#\#}P < 0.01$ vs. WT + Ang II). **c, d** NRCMs were infected with HA-Hsp90-WT (WT) or HA-Hsp90-C589A (C589A) adenovirus for 24 h and subsequently treated with Ang II (1 μM, 24 h) with or without the GSK3β inhibitor TWS119 (1 μM, 24 h). **c** The expression of eIF2Bε and p-eIF2Bε was detected by Western blotting analysis. ($n = 5$, $^{***}P < 0.001$ vs. WT, $^{\#\#}P < 0.01$ vs. WT + Ang II, $^{\$\$}P < 0.01$ vs. C589A + Ang II). **d** The mRNA levels of ANP, BNP and β-MHC were detected by RT-PCR. ($n = 5$, $^{***}P < 0.001$ vs. WT, $^{\#\#\#}P < 0.001$ vs. WT + Ang II, $^{\$\$}P < 0.01$, $^{\$\$\$}P < 0.001$ vs. C589A + Ang II).

Hsp90 promoted transforming growth factor-β type II receptor binding to Hsp90, further activating classical TGFβ/SMAD signaling in response to fibrotic stimuli [31]. Here, we provide mechanistic insight into the role of SNO-Hsp90/GSK3β signaling in cardiomyocytes during cardiac hypertrophy. GSK3β is a pivotal regulator in the development of cardiac hypertrophy. Suppression of enhanced GSK3β phosphorylation attenuates cardiac hypertrophy [32, 33]. Moreover, GSK3β is proven to be a crucial client protein of Hsp90, and Hsp90 activity is necessary for maintaining the interaction of Hsp90 and GSK3β to further regulate the phosphorylation of GSK3β [34–36]. However, whether the Hsp90/GSK3β axis functions in cardiac hypertrophy remains undetermined. We showed that

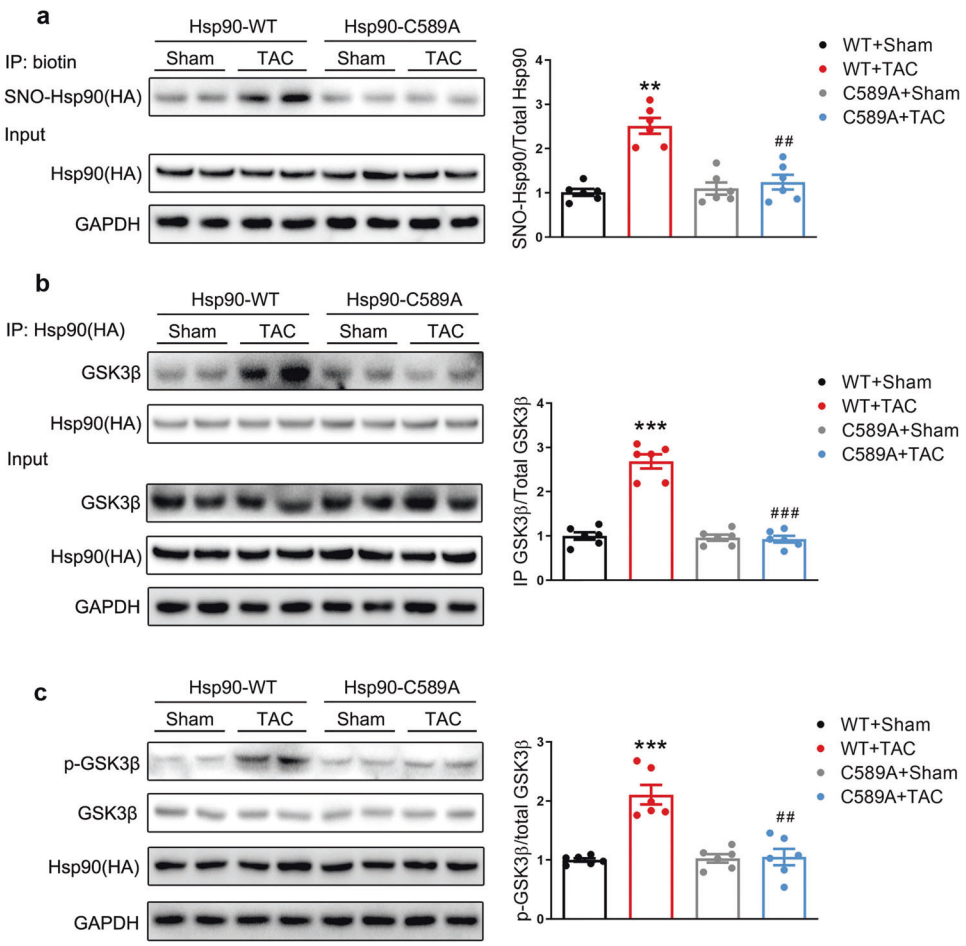

Fig. 6 Inhibition of SNO-Hsp90 by Cys589 mutation inhibits the phosphorylation of GSK3β after TAC surgery. Four-week-old C57BL/6J mice were intravenously injected with AAV9-HA-Hsp90-WT (WT) or AAV9-HA-Hsp90-C589A (C589A). After 4 weeks, these mice were subjected to sham or TAC surgery. **a** The SNO-Hsp90 levels in the myocardial tissues were detected by biotin switch assay at 4 weeks after surgery. ($n = 6$, $^{**}P < 0.01$ vs. WT + Sham, $^{\#\#}P < 0.01$ vs. WT + TAC). **b** Lysates from myocardial tissues were immunoprecipitated with an anti-HA antibody and blotted with anti-GSK3β and anti-HA antibodies at 4 weeks after surgery. An aliquot of total lysate was analyzed for GSK3β and HA expression. ($n = 6$, $^{***}P < 0.001$ vs. WT + Sham, $^{\#\#\#}P < 0.001$ vs. WT + TAC). **c** The levels of GSK3β and p-GSK3β in the myocardial tissues were detected by Western blotting analysis at 4 weeks after surgery. ($n = 6$, $^{***}P < 0.001$ vs. WT + Sham, $^{\#\#}P < 0.01$ vs. WT + TAC).

the SNO-Hsp90 at Cys589 in cardiomyocytes enhanced the interaction of GSK3β and Hsp90 to facilitate the phosphorylation of GSK3β under hypertrophic stimuli, revealing a novel regulatory mechanism for GSK3β activity. Moreover, the inhibition of SNO-Hsp90 by Cys589 mutation was able to depress GSK3β phosphorylation to alleviate cardiac hypertrophy both in vitro and in vivo, providing a therapeutic strategy for pathological cardiac hypertrophy.

NO, as a gasotransmitter, is a highly reactive signaling molecule and an important modulator in the cardiovascular system. Recent studies have proved that NO can nitrosylate cysteines in several proteins to alter their activity and then regulate cardiac and vascular function [5, 14, 37]. NO derived from three isoforms of NOS (nNOS, iNOS and eNOS) can induce protein SNO [38], while Trx and GSNOR are the other two important enzymes known to affect the SNO of targeted proteins in a denitrosylation manner [39–41]. We previously reported that the aberrant SNO of different proteins during cardiac remodeling was disparate in cardiomyocytes and cardiac fibroblasts [6, 42]. Interestingly, we showed here that the elevated SNO-Hsp90 levels were due to the down-regulated expression of GSNOR in cardiomyocytes, while it was induced by upregulated iNOS expression in cardiac fibroblasts under pathological conditions according to our recent study [31]. These results suggest the parallel regulatory mechanism of SNO in different cell types during pathological heart remodeling: GSNOR acts as a vital regulator of SNO in cardiomyocytes, and iNOS dominantly induces SNO in cardiac fibroblasts; these mechanisms help to understand the intricate pathogenesis of cardiac remodeling.

Taken together, these results provide evidence that SNO-Hsp90 at Cys589 enhances the interaction of GSK3β and Hsp90, subsequently promoting GSK3β phosphorylation to aggravate cardiac hypertrophy. These findings indicate that intervention with SNO-Hsp90 may be a therapeutic strategy for cardiac hypertrophy and heart failure.

ACKNOWLEDGEMENTS

This work was supported by grants from the National Natural Science Foundation of China (grant nos. 82030013, 82070278, 91639204, 81870183), National Key Research and Development Program of China (2019YFA0802704) and China Postdoctoral Science Foundation (2020M681667).

AUTHOR CONTRIBUTIONS

YJ, LPX and ZRH designed the research; SZ and LPX wrote the paper; SZ, TYS, ZYW, JG and JWC performed the in vitro experiments; SZ, TYS and LLH performed in vivo research and SZ and TYS analyzed data.

ADDITIONAL INFORMATION

Supplementary information The online version contains supplementary material available at https://doi.org/10.1038/s41401-021-00828-9.

Competing interests: The authors declare no competing interests.

REFERENCES

1. Nakamura M, Sadoshima J. Mechanisms of physiological and pathological cardiac hypertrophy. Nat Rev Cardiol. 2018;15:387–407.
2. Ataei Ataabadi E, Golshiri K, Juttner A, Krenning G, Danser AHJ, Roks AJM. Nitric oxide-cGMP signaling in hypertension: current and future options for pharmacotherapy. Hypertension. 2020;76:1055–68.
3. Stamler JS, Simon DI, Osborne JA, Mullins ME, Jaraki O, Michel T, et al. S-nitrosylation of proteins with nitric oxide: synthesis and characterization of biologically active compounds. Proc Natl Acad Sci USA. 1992;89:444–8.
4. Gonzalez DR, Beigi F, Treuer AV, Hare JM. Deficient ryanodine receptor S-nitrosylation increases sarcoplasmic reticulum calcium leak and arrhythmogenesis in cardiomyocytes. Proc Natl Acad Sci USA. 2007;104:20612–7.
5. Pan L, Lin Z, Tang X, Tian J, Zheng Q, Jing J, et al. S-nitrosylation of plastin-3 exacerbates thoracic aortic dissection formation via endothelial barrier dysfunction. Arterioscler Thromb Vasc Biol. 2020;40:175–88.
6. Tang X, Pan L, Zhao S, Dai F, Chao M, Jiang H, et al. SNO-MLP (S-nitrosylation of muscle LIM protein) facilitates myocardial hypertrophy through TLR3 (Toll-like receptor 3)-mediated RIP3 (receptor-interacting protein kinase 3) and NLRP3 (NOD-like receptor pyrin domain containing 3) inflammasome activation. Circulation. 2020;141:984–1000.
7. Genest O, Wickner S, Doyle SM. Hsp90 and Hsp70 chaperones: collaborators in protein remodeling. J Biol Chem. 2019;294:2109–20.
8. Mollapour M, Neckers L. Post-translational modifications of Hsp90 and their contributions to chaperone regulation. Biochim Biophys Acta. 2012;1823:648–55.
9. Kovacs JJ, Murphy PJ, Gaillard S, Zhao X, Wu JT, Nicchitta CV, et al. HDAC6 regulates Hsp90 acetylation and chaperone-dependent activation of glucocorticoid receptor. Mol Cell. 2005;18:601–7.
10. Marozkina NV, Yemen S, Borowitz M, Liu L, Plapp M, Sun F, et al. Hsp 70/Hsp 90 organizing protein as a nitrosylation target in cystic fibrosis therapy. Proc Natl Acad Sci USA. 2010;107:11393–8.
11. Martinez-Ruiz A, Villanueva L, Gonzalez de Orduna C, Lopez-Ferrer D, Higueras MA, Tarin C, et al. S-nitrosylation of Hsp90 promotes the inhibition of its ATPase and endothelial nitric oxide synthase regulatory activities. Proc Natl Acad Sci USA. 2005;102:8525–30.
12. Meng G, Liu J, Liu S, Song Q, Liu L, Xie L, et al. Hydrogen sulfide pretreatment improves mitochondrial function in myocardial hypertrophy via a SIRT3-dependent manner. Br J Pharmacol. 2018;175:1126–45.
13. Zhang Y, Da Q, Cao S, Yan K, Shi Z, Miu Q, et al. Histidine triad nucleotide binding protein 1 attenuates cardiac hypertrophy via suppressing homeobox A5 expression. Circulation. 2021;144:638–54.
14. Wang W, Wang D, Kong C, Li S, Xie L, Lin Z, et al. eNOS S-nitrosylation mediated OxLDL-induced endothelial dysfunction via increasing the interaction of eNOS with betacatenin. Biochim Biophys Acta Mol Basis Dis. 2019;1865:1793–801.
15. Lin Z, Altaf N, Li C, Chen M, Pan L, Wang D, et al. Hydrogen sulfide attenuates oxidative stress-induced NLRP3 inflammasome activation via S-sulfhydrating c-Jun at Cys269 in macrophages. Biochim Biophys Acta Mol Basis Dis. 2018;1864:2890–900.
16. Benhar M, Forrester MT, Stamler JS. Protein denitrosylation: enzymatic mechanisms and cellular functions. Nat Rev Mol Cell Biol. 2009;10:721–32.
17. Liu L, Yan Y, Zeng M, Zhang J, Hanes MA, Ahearn G, et al. Essential roles of S-nitrosothiols in vascular homeostasis and endotoxic shock. Cell. 2004;116:617–28.
18. Hardt SE, Sadoshima J. Glycogen synthase kinase-3beta: a novel regulator of cardiac hypertrophy and development. Circ Res. 2002;90:1055–63.
19. Wang SB, Venkatraman V, Crowgey EL, Liu T, Fu Z, Holewinski R, et al. Protein S-nitrosylation controls glycogen synthase kinase 3beta function independent of its phosphorylation state. Circ Res. 2018;122:1517–31.
20. Okamoto S, Lipton SA. S-nitrosylation in neurogenesis and neuronal development. Biochim Biophys Acta. 2015;1850:1588–93.
21. Lima B, Forrester MT, Hess DT, Stamler JS. S-nitrosylation in cardiovascular signaling. Circ Res. 2010;106:633–46.
22. Irie T, Sips PY, Kai S, Kida K, Ikeda K, Hirai S, et al. S-nitrosylation of calcium-handling proteins in cardiac adrenergic signaling and hypertrophy. Circ Res. 2015;117:793–803.
23. Schopf FH, Biebl MM, Buchner J. The HSP90 chaperone machinery. Nat Rev Mol Cell Biol. 2017;18:345–60.
24. Xu W, Beebe K, Chavez JD, Boysen M, Lu Y, Zuehlke AD, et al. Hsp90 middle domain phosphorylation initiates a complex conformational program to recruit the ATPase-stimulating cochaperone Aha1. Nat Commun. 2019;10:2574.
25. Blank M, Mandel M, Keisari Y, Meruelo D, Lavie G. Enhanced ubiquitinylation of heat shock protein 90 as a potential mechanism for mitotic cell death in cancer cells induced with hypericin. Cancer Res. 2003;63:8241–7.
26. Ebert A, Joshi AU, Andorf S, Dai Y, Sampathkumar S, Chen H, et al. Proteasome-dependent regulation of distinct metabolic states during long-term culture of human iPSC-derived cardiomyocytes. Circ Res. 2019;125:90–103.
27. Boucherat O, Peterlini T, Bourgeois A, Nadeau V, Breuils-Bonnet S, Boilet-Molez S, et al. Mitochondrial HSP90 accumulation promotes vascular remodeling in pulmonary arterial hypertension. Am J Respir Crit Care Med. 2018;198:90–103.
28. Eschricht S, Jarr KU, Kuhn C, Lehmann L, Kreusser M, Katus HA, et al. Heat-shock-protein 90 protects from downregulation of HIF-1alpha in calcineurin-induced myocardial hypertrophy. J Mol Cell Cardiol. 2015;85:117–26.
29. Marunouchi T, Nakashima M, Ebitani S, Umezu S, Karasawa K, Yano E, et al. Hsp90 inhibitor attenuates the development of pathophysiological cardiac fibrosis in mouse hypertrophy via suppression of the calcineurin-NFAT and c-Raf-Erk pathways. J Cardiovasc Pharmacol. 2021;77:822–9.
30. Tamura S, Marunouchi T, Tanonaka K. Heat-shock protein 90 modulates cardiac ventricular hypertrophy via activation of MAPK pathway. J Mol Cell Cardiol. 2019;127:134–42.
31. Zhang X, Zhang Y, Miao Q, Shi Z, Hu L, Liu S, et al. Inhibition of HSP90 S-nitrosylation alleviates cardiac fibrosis via TGFbeta/SMAD3 signaling pathway. Br J Pharmacol. 2021;178:4608–25.
32. Yan L, Wei X, Tang QZ, Feng J, Zhang Y, Liu C, et al. Cardiac-specific mindin overexpression attenuates cardiac hypertrophy via blocking AKT/GSK3beta and TGF-beta1-Smad signalling. Cardiovasc Res. 2011;92:85–94.
33. Gao XQ, Zhang YH, Liu F, Ponnusamy M, Zhao XM, Zhou LY, et al. The piRNA CHAPIR regulates cardiac hypertrophy by controlling METTL3-dependent N(6)-methyladenosine methylation of Parp10 mRNA. Nat Cell Biol. 2020;22:1319–31.
34. Lochhead PA, Kinstrie R, Sibbet G, Rawjee T, Morrice N, Cleghon V. A chaperone-dependent GSK3beta transitional intermediate mediates activation-loop autophosphorylation. Mol Cell. 2006;24:627–33.
35. Banz VM, Medova M, Keogh A, Furer C, Zimmer Y, Candinas D, et al. Hsp90 transcriptionally and post-translationally regulates the expression of NDRG1 and maintains the stability of its modifying kinase GSK3beta. Biochim Biophys Acta. 2009;1793:1597–603.
36. Xu Q, Tu J, Dou C, Zhang J, Yang L, Liu X, et al. HSP90 promotes cell glycolysis, proliferation and inhibits apoptosis by regulating PKM2 abundance via Thr-328 phosphorylation in hepatocellular carcinoma. Mol Cancer. 2017;16:178.
37. Majumdar U, Manivannan S, Basu M, Ueyama Y, Blaser MC, Cameron E, et al. Nitric oxide prevents aortic valve calcification by S-nitrosylation of USP9X to activate NOTCH signaling. Sci Adv. 2021;7:eabe3706.
38. Farah C, Michel LYM, Balligand JL. Nitric oxide signalling in cardiovascular health and disease. Nat Rev Cardiol. 2018;15:292–316.
39. Chen G, An N, Ye W, Huang S, Chen Y, Hu Z, et al. bFGF alleviates diabetes-associated endothelial impairment by downregulating inflammation via S-nitrosylation pathway. Redox Biol. 2021;41:101904.
40. Liu L, Hausladen A, Zeng M, Que L, Heitman J, Stamler JS. A metabolic enzyme for S-nitrosothiol conserved from bacteria to humans. Nature. 2001;410:490–4.
41. Yi W, Zhang Y, Liu B, Zhou Y, Liao D, Qiao X, et al. Protein S-nitrosylation regulates proteostasis and viability of hematopoietic stem cell during regeneration. Cell Rep. 2021;34:108922.
42. Zhou M, Chen JY, Chao ML, Zhang C, Shi ZG, Zhou XC, et al. S-nitrosylation of c-Jun N-terminal kinase mediates pressure overload-induced cardiac dysfunction and fibrosis. Acta Pharmacol Sin. 2021. https://doi.org/10.1038/s41401-021-00674-9. [Online ahead of print].